Research Article | Vol. 10, No. 4 | 1 Apr 2019 | BIOMEDICAL OPTICS EXPRESS 2141
Biomedical Optics EXPRESS

Imaging the brain in 3D using a combination of CUBIC and immunofluorescence staining

YANGYANG XU,[1] PENG LI,[1] MENGQI WANG,[1] JIE ZHANG,[2] AND WEI WANG[1,*]

[1]*Department of Neurosurgery, West China Hospital of Sichuan University, Guoxue Street 37, Chengdu, Sichuan 610041, China*
[2]*Key Laboratory of Transplant Engineering and Immunology, Ministry of Health, Regenerative Medicine Research Center, West China Hospital of Sichuan University, Chengdu, Sichuan 610041, China*
[*]*wcnsww@163.com*

Abstract: Three-dimensional (3D) high-resolution imaging can help us better understand the brain, and CUBIC is a powerful technique to render the brain transparent, thus benefiting 3D imaging. In this study, we combined CUBIC with immunofluorescence staining (IFS) and successfully acquired 3D high-resolution images of cerebral vessels, astrocytes, dopaminergic neurons and pericytes, providing us abundant information about the change in spatial frequency content for cellular scale features. Additionally, we found that a longer duration of antibody incubation produced deeper staining. Our study indicates the broad application prospects of IFS-based CUBIC for studying specific cerebral structures and diseases related to alterations of these structures.

1. Introduction

The sophisticated neural network is the structural foundation of the highly coordinated cerebral function. Specific neural networks perform specific functions, and different neural networks are intricately linked, together participating in the regulation of movement, sensation, cognition, emotion and memory [1]. To obtain a better understanding of cerebral function, we must first have a full picture of the cerebral structure. However, to acquire a three-dimensional (3D) high-resolution image of the brain has been a challenge confronting scientists. Although the development of imaging techniques such as computed tomography and magnetic resonance imaging enables us to easily build a 3D image of the whole brain, resolution of the images is far from the cellular level and thus lacks some critical microscopic information. In contrast, conventional histopathological techniques based on slices can offer us high-resolution images, but the limited thickness of slices prevents us from acquiring more information on the z-axis.

Recent years have witnessed the rapid development of brain-clearing techniques [2]. By combining with confocal microscopy, light sheet fluorescence microscopy or two-photon microscopy, 3D high-resolution images of the brain can be easily obtained, thus benefiting researches on the relationship between cerebral structure and function. Among numerous brain-clearing techniques, CUBIC is a rather powerful one [3,4]. CUBIC is an acronym of the term “clear, unobstructed brain imaging cocktails and computational analysis”, which was first introduced by Susaki et al. in 2014 [3]. By removing lipids and homogenizing the refractive indices, the whole mouse brain can be made visually transparent with CUBIC within 14 d [4]. The simple clearing procedure, excellent clearing effect in a relatively short time period and outstanding ability for fluorescence preservation represent the advantages of CUBIC, making it a popular option among labs [5–8]. However, although Susaki et al. successfully cleared and imaged the whole mouse brain with CUBIC, their results were mainly based on transgenic mice with endogenous fluorescence, while the most commonly

#342859 https://doi.org/10.1364/BOE.10.002141
Journal © 2019 Received 21 Aug 2018; revised 12 Mar 2019; accepted 13 Mar 2019; published 1 Apr 2019

Biomedical Optics EXPRESS

used method to identify a specific cerebral structure, immunofluorescence staining (IFS), was not explicitly described and fully explored in their papers. Following Susaki et al.'s ptotocol, some researchers have tried to extend the application of CUBIC by combining it with IFS with encouraging results [9,10], but the literature is still very limited and the methods used by different authors vary, limiting choices for references.

In the present study, CUBIC and IFS were combined and performed with appropriate modifications according to our experimental conditions. 3D high-resolution images of cerebral vessels, astrocytes, dopaminergic neurons and pericytes were successfully acquired on cleared brain with confocal microscopy imaging. After 3D rendering with Imaris, the stereoscopic morphology of different structures and the spatial relationship between different structures became easily understood and apparent. Our study represents an extension of the original CUBIC technique, demonstrating the potentially broad application prospects of IFS-based CUBIC for studying specific cerebral structures and diseases related to alterations of these structures.

2. Materials and methods

2.1 Mice

Adult C57BL/6 mice (6 w of age, Huafukang Animal Centre, Beijing, China) were used in this study. All procedures were performed in compliance with local regulations of animal welfare and experimental ethics. The study was approved by West China Hospital of Sichuan University Biomedical Research Ethics Committee.

2.2 Reagents and antibodies

The reagents for CUBIC are listed in Table 1. Reagent-1 is composed of urea, quadrol, Triton X-100 and dH_2O. Reagent-2 is composed of urea, sucrose, triethanolamine and dH_2O. 1/2-Reagent-1 is a mixture of reagent-1 and dH_2O (1:1). 1/2-Reagent-2 is a mixture of reagent-2 and PBS (1:1). Reagent-1, Reagent-2, 1/2-Reagent-1 and 1/2-Reagent-2 were prepared based on the original protocol [4]. Dextran-FITC (2000kDa, Sigma-Aldrich, FD2000S) was utilized to label the cerebral vessels of C57BL/6 mice. Primary antibodies included anti-Tyrosine Hydroxylase (TH) (Abcam, ab6211, 1:1000), anti-GFAP (GFAP) (Abcam, ab53554; 1:500), anti-PDGF Receptor beta (PDGFRβ) (Abcam, ab32570, 1:200), anti-desmin (desmin) (Abcam, ab32362, 1:200). Secondary antibodies included Rabbit anti-Goat-Alexa Fluor 647 (Jackson ImmunoResearch, 305-605-003, 1:200), Goat anti-Rabbit-Alexa Fluor 647 (Jackson ImmunoResearch, 111-605-003, 1:200) and Donkey anti-Rabbit-Rhodamine (Jackson ImmunoResearch, 711-025-152, 1:200).

Table 1. Reagents for CUBIC

Name of reagents	Company	CAT #
Sucrose	Sigma-Aldrich	V900116
Triethanolamine	Sigma-Aldrich	V900257
Urea	Sigma-Aldrich	U5378
Qaudrol	Sigma-Aldrich	122262
Triton X-100	Sigma-Aldrich	T8787

2.3 Heart perfusion and brain collection

Dextran-FITC (6 μg/μl, 100 μl) was injected through the tail vein and allowed to circulate for 10 min to label the cerebral vessels. The mouse was anesthetized with 1% pentobarbital sodium (3 ml/kg, ip) and transcardially perfused with 4°C PBS (20 ml) to flush out the circulating blood, followed by perfusion with 4% PFA (20 ml) to fix the brain. Finally, the brain was excised, collected and then postfixed in 4% PFA at 4°C for 12 h.

Biomedical Optics EXPRESS

2.4 Clearing the brain with CUBIC

The CUBIC clearing procedure was performed with appropriate modification according to our experimental conditions and objectives. Both the whole brain and thick brain blocks were cleared in this study. After fixation with 4% PFA overnight, brain samples were washed with PBS for 1 h*3 with shaking at room temperature (RT). For thick brain blocks, the whole brain was coronally cut into 3 mm-thick blocks after the washing step. The samples were then cleared with 1/2-Reagent-1 with shaking at a speed of 60 rpm at 37°C for 3 h. Reagent-1 was applied for further clearing under the same conditions and replaced every two days until a satisfying optical transparency was achieved. The sample was then washed with PBS with soft shaking at RT for 1 h*3. Then, 1/2-Reagent-2 was applied to clear the sample with shaking at 60 rpm at 37°C for 24 h. Reagent-2 was then applied for further clearing and replaced every two days until a satisfying optical transparency was achieved. Cleared samples were stored in Reagent-2 at 4°C until imaging. All clearing procedures were performed in dark conditions to avoid fluorescence bleaching.

2.5 Immunofluorescence staining (IFS)

IFS was conducted on thick brain blocks and performed in the interval between clearing with Reagent-1 and Reagent-2. After clearing with Reagent-1, the sample was washed with PBS for 1 h*3, and then blocked with 5% BSA with shaking at 60 rpm at 37°C for 3 h. Subsequently, the sample was incubated with primary antibodies (diluted in 5% BSA) with shaking at 60 rpm at 37°C for 24 h. The sample was washed with PBS with shaking at RT for 1 h*3. Corresponding secondary antibodies (diluted in 5% BSA) were applied to the sample under the same conditions as the primary antibody incubations. Then, the sample was washed with PBS again for 1 h*3. For double staining, we first incubated the sample with TH and the corresponding secondary antibody (Donkey anti-Rabbit-Rhodamine). After washing with PBS, the second round of staining with GFAP and the corresponding secondary antibody (Rabbit anti-Goat-Alexa Fluor 647) was performed in the same way. Once IFS was completed, clearing with Reagent-2 continued as described above.

2.6 Image acquisition

Samples were placed in a glass-bottom dish and imaged with inverted confocal microscopy (Nikon A1plus) using a Plan Apo VC 20X/0.75 DIC N2 objective or a Plan Apo VC 10x/0.45 DIC L objective (Fig. 1(C)). To acquire the z-stack profile, images were obtained at a thickness of 1 μm per step, and imaging parameters were linearly adjusted to obtain images of the best quality at each step. For each area of interest, imaging continued until the target signal disappeared. All images were processed with Imaris 9.0.1 (Bitplane, Switzerland), and the Surfaces visualization was used for 3D rendering. The imaging depth and the staining depth was determined by measuring the distance along the z-axis between the first layer of the 3D image and the layer where the target signal had just disappeared. The mean grey value was quantified with image-pro plus 6.0 (Media Cybernetics, the USA) as an indication of fluorescence intensity of images. The relative fluorescence intensity was defined as a ratio of fluorescence intensity of the image to that of the first layer of the 3D image. Therefore, relative fluorescence intensity of the first layer of the 3D image was normalized as 1.0.

2.7 Statistical analysis

Differences in staining depth among different incubation time were compared using ANOVA. Multiple pairwise comparisons were performed using uncorrected Fisher's LSD. A confidence interval of 95% was adopted for all tests. All analyses were conducted with GraphPad Prism7. Quantified data are presented as mean ± SD.

Biomedical Optics EXPRESS

3. Results

The original CUBIC protocol was modified according to our experimental conditions and objectives, through which, we successfully cleared the whole mouse brain and thick brain blocks. It took 10 d and 6 d to clear the whole brain and thick brain blocks with the modified protocol, respectively (Fig. 1(A)). Compared with the uncleared brain, the cleared brain exhibited an excellent clearing effect but appeared slightly swollen (Fig. 1(B)). Dextran-FITC was applied to some mice to label cerebral vessels. To investigate how CUBIC could help us look more deeply into the brain, we imaged cerebral vessels before and after clearing, and the maximum imaging depths before and after clearing were 106.5 μm (Fig. 1(D)) and 1200 μm (Fig. 1(E)), respectively.

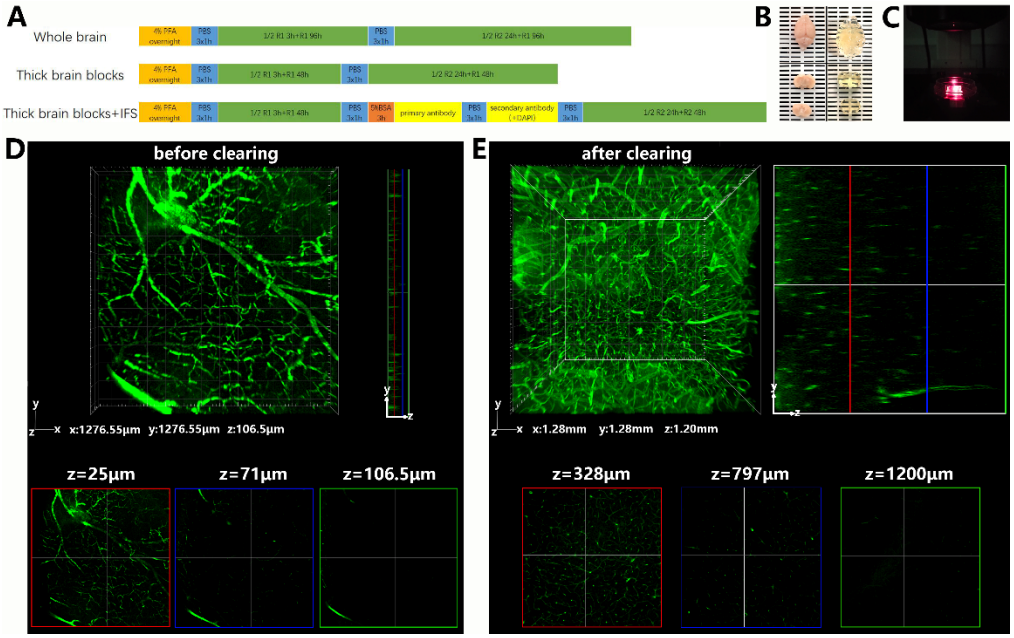

Fig. 1. CUBIC significantly increased the transparency of the brain and the imaging depth. A: The pipeline of the modified CUBIC protocol; B: Macro images of the whole brain and thick brain blocks before and after clearing; C: The sample was placed in a glass-bottom dish and imaged with inverted confocal microscopy; The maximum imaging depths of cerebral vessels were 106.5 μm in uncleared brain blocks (D) and 1.2 mm in cleared brain blocks (E) (imaged with a Plan Apo VC 10x/0.45 DIC L objective).

IFS was conducted in the interval between clearing with Reagent-1 and Reagent-2 on thick brain blocks. To investigate the compatibility of CUBIC with different antibodies, we adopted a three-hour antibody incubation scheme to test GFAP, TH, desmin and PDGFRβ on cleared brain blocks whose vessels were stained by Dextran-FITC. All the corresponding target antigens were well stained (Figs. 2(A), 2(B), 2(C), and 2(D)). Astrocytes, dopaminergic neurons, and pericytes and their proximity to cerebral vessels were clearly observed in 3D images after 3D rendering with Imaris (Figs. 2(A)', 2(B)', 2(C)', and 2(D)'). The staining depths of GFAP, TH, Desmin and PDGFRβ staining in the three-hour incubation scheme were 172 ± 17 μm, 137 ± 10 μm, 201 ± 14 μm and 242 ± 20 μm, respectively (n = 3). To investigate whether CUBIC is compatible with repetitive IFS, we conducted double staining with GFAP and TH, and both astrocytes and dopaminergic neurons were well stained in the same 3D image (Fig. 2(E)). After 3D rendering with Imaris, the spatial relationship among astrocytes, dopaminergic neurons and cerebral vessels became more easily understood and apparent (Fig. 2(E)').

Biomedical Optics EXPRESS

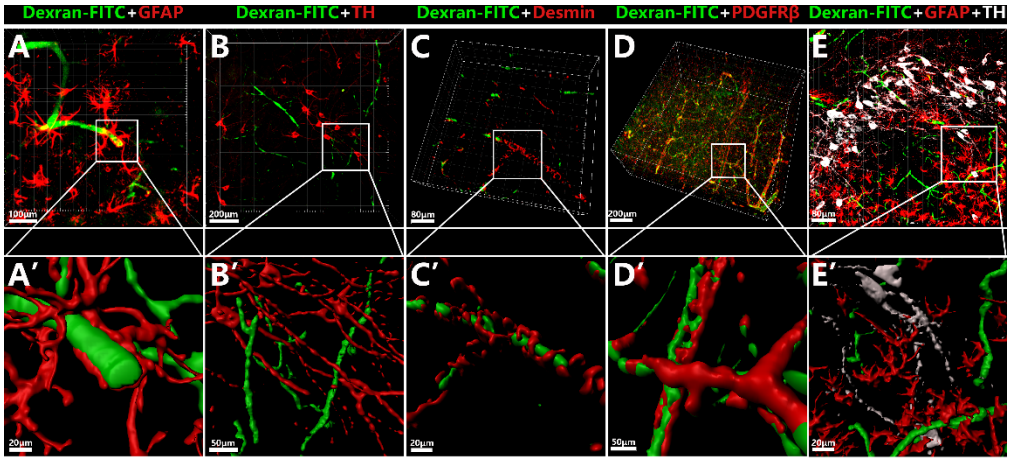

Fig. 2. IFS conducted on cleared samples. A, B, C and D demonstrate the GFAP (imaged with a Plan Apo VC 20X/0.75 DIC N2 objective, zoom2), TH (imaged with a Plan Apo VC 20X/0.75 DIC N2 objective, zoom1), desmin (imaged with a Plan Apo VC 20X/0.75 DIC N2 objective, zoom2.469) and PDGFRβ (imaged with a Plan Apo VC 20X/0.75 DIC N2 objective, zoom1) staining; A', B', C' and D' demonstrate images after 3D rendering with Imaris. E demonstrates the result of double staining with GFAP and TH, and E' demonstrates the image after 3D rendering with Imaris.

To further investigate whether longer durations of antibody incubation can produce deeper staining, the time of GFAP and PDGFRβ antibody incubation was extended. When the antibody incubation time was extended to 24 h, the GFAP and PDGFRβ staining depth reached 383 ± 64 μm and 425 ± 24 μm (n = 3) (Figs. 3(A) and 3(C)), and when the incubation time was extended to 3 d,-the GFAP and PDGFRβ staining depth reached 575 ± 57 μm and 657 ± 17 μm (Figs. 3(B) and 3(D)), respectively (n = 3). The difference in staining depths among different incubation time was statistically significant (Fig. 3(E)). At the same time, a significant downward trend of fluorescence intensity with depth was also observed (Fig. 3(F)). In this section, cell nuclei were stained with DAPI at the same time. To shorten the entire procedure as much as possible, DAPI and secondary antibodies were incubated together, which proved workable.

Biomedical Optics EXPRESS

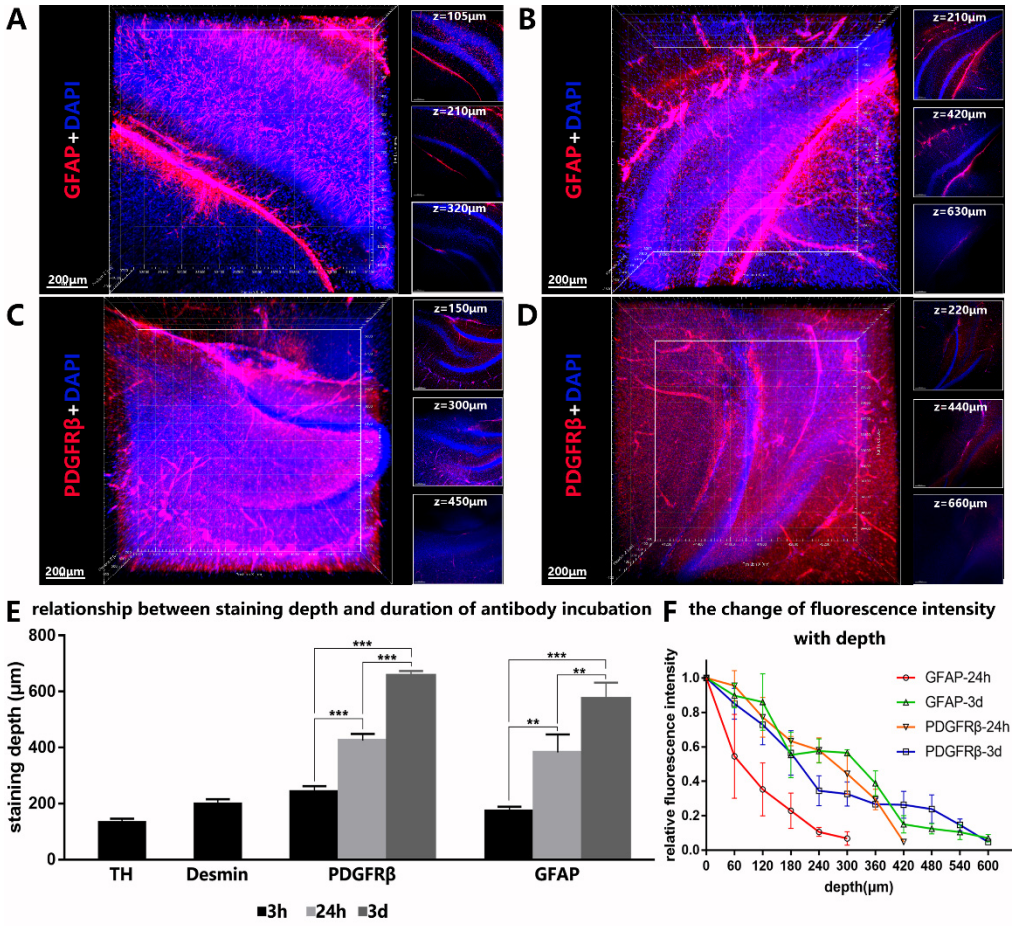

Fig. 3. A longer duration of antibody incubation produced deeper staining. A and B demonstrate IFS with GFAP for an incubation duration of 24 h (z = 322 μm) and 3 d (z = 640 μm), respectively. C and D demonstrate IFS with PDGFRβ for an incubation duration of 24 h (z = 451 μm) and 3 d (z = 670 μm), respectively (imaged with a Plan Apo VC 10x/0.45 DIC L objective). E illustrates the relationship between staining depth and antibody incubation time. ** indicates $p<0.005$. *** indicates $p<0.0001$. F illustrates the reduction of fluorescence intensity with depth.

4. Discussion

Neurons and glial cells are the main cellular components of the brain. The blood-brain barrier (BBB) helps maintain homeostasis of the brain and is composed of endothelium, pericytes and astrocytes [11]. In the present study, we used astrocytes as the representative of glial cells, dopaminergic neurons as the representative of neurons and pericytes as the representative of the BBB and successfully acquired 3D high-resolution images of these structures through IFS-based CUBIC. The spatial distribution of structures and the spatial relationship among different structures was clearly seen in the 3D images. Our study suggests the broad application prospect of IFS-based CUBIC for investigating various cerebral structures and diseases related to alterations of these structures.

The clearing effects of CUBIC were validated by visual inspection and confocal imaging in the present study. An obvious transparency was achieved after clearing with CUBIC for 10 d for the whole brain and for 6 d for the 3 mm-thick brain blocks. Meanwhile, tissue expansion was also observed after clearing in the present study, which was consistent with previous studies [9]. The imaging depth of confocal microscopy is usually limited to

Biomedical Optics EXPRESS

approximately 100 μm in uncleared tissues, but can be largely increased after tissue clearing [4]. In our study, the maximum imaging depth was increased by more than 10 times after clearing, which was comparable to the study performed on mouse hearts by Nehrhoff et al. [7]. The excellent clearing effect in a relatively short time period represents one advantage of CUBIC [12–14]. By cutting the brain into thick blocks, the entire clearing procedure can be further shortened. In the original protocol, the authors recommended that the procedure be modified according to the experimental purpose and a one-step immersion in Reagent-1 for 1-3 d should be sufficient for some studies [4]. Likewise, the size of tissues can be determined based on the experimental purpose to achieve the best results in the shortest time frame. In the study conducted by Liang et al. [10], the mouse brain was sagittally halved before clearing with CUBIC. In a study performed on the chicken embryo brain [10], 1-mm thick sections were adopted for some experiments.

CUBIC demonstrated excellent compatibility with IFS [5,7–10,12,14–17]. Four antibodies were tested in this study, all of which well stained the target antigens. Four bands of fluorescence (405 nm, 488 nm, 550 nm and 647 nm) were successfully applied in our study. Other fluorochromes, such as RedDots [5], mCherry, YFP [3] and propidium iodide [4], have also demonstrated satisfying staining effects in tissues cleared with CUBIC, demonstrating the scalability of fluorescence preservation of CUBIC. Furthermore, repetitive IFS was feasible in tissues cleared with CUBIC. By staining different structures in the same 3D image, the spatial relationship between them can be seen more clearly, thus providing us with plenty of microscopic information.

Compared with the imaging depth, the penetration depth of antibodies represents a limitation for detecting deeper structures. The imaging depth by confocal microscopy can easily reach over 1 mm after clearing with CUBIC, but the penetration depth of antibodies is usually limited [7,9]; however, CUBIC itself can increase the permeability of samples for antibodies to penetrate inside by removing lipids [3,7,9]. Increasing the penetration depth of antibodies into cleared tissues has become a focus of investigation, and several techniques have been developed to do so. By applying external pressure, the ACT-PRESTO technique can markedly speed up-antibody penetration into cleared samples, thus increasing the staining depth [15]. Kim et al. introduced a method called stochastic electrotransport to accelerate the antibody incubation procedure in cleared samples [18]. By synchronizing labeling reactions, the SWITCH technique can significantly improve the penetration depth of antibodies [19]. However, all these techniques were combined with clearing techniques other than CUBIC. For CUBIC, no such techniques are presently available, but one can increase the penetration depth of antibodies by extending the incubation time or tailoring the sample size. By extending the incubation time to weeks, the whole mouse brain can be fully stained [10,20]. Although this process is time-consuming, increasing the staining depth by extending the incubation time is a simple and effective approach at present, especially for CUBIC that possesses an excellent capacity for fluorescence preservation. Of course, spending several weeks to stain the whole brain may not be cost-effective for some researchers. Therefore, the incubation time and the staining depth should be balanced to accomplish the experimental objectives in a reasonable time frame. Reducing the volume of samples by dividing the brain into thick blocks is another way to increase the staining depth of antibodies [9], because antibodies entering the tissue from different directions can meet in a shorter amount of time in a thick brain block than in the whole brain. Indeed, imaging a whole cleared mouse brain is impractical in many labs due to the lack of light sheet microscopy. Instead, as far as we know, labs are more often equipped with confocal microscopy. Confocal microscopy can provide us with 3D high-resolution images, but its imaging speed is much slower than that of light sheet microscopy. To image a whole mouse brain with confocal microscopy may take approximately 50 d [2], which is rather unpractical. In this case, it is feasible to clear and stain a thick brain block with CUBIC and image it with confocal microscopy, just as we did in this study.

Biomedical Optics EXPRESS

5. Conclusion

CUBIC is a simple and practical technique to clear both the whole brain and thick brain blocks and is well compatible with IFS. IFS conducted on cleared samples is similar to that conducted on conventional thin slices. The staining depth of antibodies can be increased by extending the incubation time. Through staining specific antigens in cleared brains, we can obtain abundant microscopic information about the central nervous system, which may advance our understanding of the central nervous system. For labs who decide to perform tissue clearing experiments, the CUBIC technique is a good choice.

Funding

National Natural Science Foundation of China (81271408); Sichuan Province Science and Technology Support Program (2018FZ0034); 135 Project of Outstanding Development of West China Hospital, Sichuan University (ZY2017307).

Acknowledgments

We thank Lin Bai for support with confocal image acquisition.

Disclosures

The authors declare that there are no conflicts of interest related to this article.

References

1. K. J. Friston, "Functional and effective connectivity: a review," Brain Connect. **1**(1), 13–36 (2011).
2. D. S. Richardson and J. W. Lichtman, "Clarifying Tissue Clearing," Cell **162**(2), 246–257 (2015).
3. E. A. Susaki, K. Tainaka, D. Perrin, F. Kishino, T. Tawara, T. M. Watanabe, C. Yokoyama, H. Onoe, M. Eguchi, S. Yamaguchi, T. Abe, H. Kiyonari, Y. Shimizu, A. Miyawaki, H. Yokota, and H. R. Ueda, "Whole-brain imaging with single-cell resolution using chemical cocktails and computational analysis," Cell **157**(3), 726–739 (2014).
4. E. A. Susaki, K. Tainaka, D. Perrin, H. Yukinaga, A. Kuno, and H. R. Ueda, "Advanced CUBIC protocols for whole-brain and whole-body clearing and imaging," Nat. Protoc. **10**(11), 1709–1727 (2015).
5. S. I. Kubota, K. Takahashi, J. Nishida, Y. Morishita, S. Ehata, K. Tainaka, K. Miyazono, and H. R. Ueda, "Whole-Body Profiling of Cancer Metastasis with Single-Cell Resolution," Cell Reports **20**(1), 236–250 (2017).
6. P. Matryba, L. Bozycki, M. Pawłowska, L. Kaczmarek, and M. Stefaniuk, "Optimized perfusion-based CUBIC protocol for the efficient whole-body clearing and imaging of rat organs," J. Biophotonics **11**(5), e201700248 (2018).
7. I. Nehrhoff, D. Bocancea, J. Vaquero, J. J. Vaquero, J. Ripoll, M. Desco, and M. V. Gómez-Gaviro, "3D imaging in CUBIC-cleared mouse heart tissue: going deeper," Biomed. Opt. Express **7**(9), 3716–3720 (2016).
8. S. Nojima, E. A. Susaki, K. Yoshida, H. Takemoto, N. Tsujimura, S. Iijima, K. Takachi, Y. Nakahara, S. Tahara, K. Ohshima, M. Kurashige, Y. Hori, N. Wada, J. I. Ikeda, A. Kumanogoh, E. Morii, and H. R. Ueda, "CUBIC pathology: three-dimensional imaging for pathological diagnosis," Sci. Rep. **7**(1), 9269 (2017).
9. M. V. Gómez-Gaviro, E. Balaban, D. Bocancea, M. T. Lorrio, M. Pompeiano, M. Desco, J. Ripoll, and J. J. Vaquero, "Optimized CUBIC protocol for three-dimensional imaging of chicken embryos at single-cell resolution," Development **144**(11), 2092–2097 (2017).
10. H. Liang, H. Wang, S. Wang, R. Francis, G. Paxinos, and X. Huang, "3D imaging of PSD-95 in the mouse brain using the advanced CUBIC method," Mol. Brain **11**(1), 50 (2018).
11. Z. Zhao, A. R. Nelson, C. Betsholtz, and B. V. Zlokovic, "Establishment and Dysfunction of the Blood-Brain Barrier," Cell **163**(5), 1064–1078 (2015).
12. J. Seo, M. Choe, and S. Y. Kim, "Clearing and Labeling Techniques for Large-Scale Biological Tissues," Mol. Cells **39**(6), 439–446 (2016).
13. M. Frétaud, L. Rivière, É. Job, S. Gay, J. J. Lareyre, J. S. Joly, P. Affaticati, and V. Thermes, "High-resolution 3D imaging of whole organ after clearing: taking a new look at the zebrafish testis," Sci. Rep. **7**(1), 43012 (2017).
14. M. Orlich and F. Kiefer, "A qualitative comparison of ten tissue clearing techniques," Histol. Histopathol. **33**(2), 181–199 (2018).
15. E. Lee, J. Choi, Y. Jo, J. Y. Kim, Y. J. Jang, H. M. Lee, S. Y. Kim, H. J. Lee, K. Cho, N. Jung, E. M. Hur, S. J. Jeong, C. Moon, Y. Choe, I. J. Rhyu, H. Kim, and W. Sun, "ACT-PRESTO: Rapid and consistent tissue clearing and labeling method for 3-dimensional (3D) imaging," Sci. Rep. **6**(1), 18631 (2016).
16. B. Lloyd-Lewis, F. M. Davis, O. B. Harris, J. R. Hitchcock, F. C. Lourenco, M. Pasche, and C. J. Watson, "Imaging the mammary gland and mammary tumours in 3D: optical tissue clearing and immunofluorescence methods," Breast Cancer Res. **18**(1), 127 (2016).

Biomedical Optics EXPRESS

17. F. M. Davis, B. Lloyd-Lewis, O. B. Harris, S. Kozar, D. J. Winton, L. Muresan, and C. J. Watson, "Single-cell lineage tracing in the mammary gland reveals stochastic clonal dispersion of stem/progenitor cell progeny," Nat. Commun. **7**(1), 13053 (2016).
18. S. Y. Kim, J. H. Cho, E. Murray, N. Bakh, H. Choi, K. Ohn, L. Ruelas, A. Hubbert, M. McCue, S. L. Vassallo, P. J. Keller, and K. Chung, "Stochastic electrotransport selectively enhances the transport of highly electromobile molecules," Proc. Natl. Acad. Sci. U.S.A. **112**(46), E6274–E6283 (2015).
19. E. Murray, J. H. Cho, D. Goodwin, T. Ku, J. Swaney, S. Y. Kim, H. Choi, Y. G. Park, J. Y. Park, A. Hubbert, M. McCue, S. Vassallo, N. Bakh, M. P. Frosch, V. J. Wedeen, H. S. Seung, and K. Chung, "Simple, Scalable Proteomic Imaging for High-Dimensional Profiling of Intact Systems," Cell **163**(6), 1500–1514 (2015).
20. K. Chung, J. Wallace, S. Y. Kim, S. Kalyanasundaram, A. S. Andalman, T. J. Davidson, J. J. Mirzabekov, K. A. Zalocusky, J. Mattis, A. K. Denisin, S. Pak, H. Bernstein, C. Ramakrishnan, L. Grosenick, V. Gradinaru, and K. Deisseroth, "Structural and molecular interrogation of intact biological systems," Nature **497**(7449), 332–337 (2013).